Journal of Animal and Veterinary Advances 10 (1): 55-59, 2011
ISSN: 1680-5593

Computed Tomographic Imaging of Vesicular Glands in Rabbits

[1]R. Dimitrov, [3]Y. Toneva, [2]D. Vladova, [1]K. Stamatova and [2]M. Stefanov
[1]Department of Veterinary Anatomy, Histology and Embryology,
Faculty of Veterinary Medicine,
[2]Department of Animal Morphology, Physiology and Nutrition,
Faculty of Agriculture,
[3]Department of Medical Physics, Biophysics and Diagnostic Imaging,
Faculty of Medicine, Trakia University, 6000 Stara Zagora, Bulgaria

Abstract: The study was carried out with the purpose to demonstrate the anatomo-topographic features of rabbit vesicular glands by computed axial tomography imaging (CT). Eight sexually matured, clinically healthy male white New Zealand rabbits, 12 months of age and weighing 2.8-3.2 kg were used. CT scans of the pelvis were performed in the transverse planes from the seventh Lumbar (L7) vertebra to the first Sacral vertebra (S1), with a section thickness of 2 mm. The cranial border of the vesicular glands was visualized in the transverse plane between L7 and S1 while the caudal part of the glands was observed in scans of the pelvic inlet in the transverse plane through the caudal part of S1. In the transverse scans of the pelvic inlet halfway S1, the vesicular glands appeared as transversely ovoid, homogeneous and relatively hypodense structures as compared to the adjacent soft tissues. The glandular areas were relatively hypodense compared to the urethral and rectal walls. The density of the rabbit vesicular glands was that of the soft tissues, ranging from 31±0.33 HU in precontrast imaging and 78±0.33 HU in postcontrast imaging.

Key words: Vesicular glands, imaging anatomy, rabbit, hypodense, Transversely ovoid, sacral vertebra

INTRODUCTION

In the conventional topographic anatomy, the rabbit vesicular glands are described as lobular organs with an irregular shape and a variable size, depending on the amount of the secretory product presented in the glandular cavities (Del Sol and Vasquez, 2003; Holtz and Foote, 1978; Mollineau *et al*., 2006; McCracken *et al*., 2008). The cranial part of the dorsal surface of the glands extends to the rectum. From the caudal glandular surface which extends to the cranial part of the prostate gland, emerge the ejaculatory ducts of the glands. The ventral surface of the vesicular glands is connected to the ampullae of the deferent ducts. The vesicular glands are covered by a capsule consisting of smooth muscle layers.

Computed axial Tomography (CT) imaging studies of domestic animals vesicular glands are few. Archana *et al*. (2009) who investigated vesicular glands in the Gaddi goat have demonstrated that these glands are located dorsolaterally to the urinary bladder neck and lateral to ampullae of the deferent ducts. In young goats the glands were small and not lobulated whereas in adults they changed in shape and became larger and lobulated. In contrast, in human medicine studies on both normal and pathological vesicular glands are plenty (Lantz *et al*., 1981; Silverman *et al*., 1985; Kang *et al*., 1989; Kuyumcuoglu *et al*., 1991; Munkelwitz *et al*., 1997; Altunrende *et al*., 2004; Lee *et al*., 2007; Lawson and Macdougall, 1965).

The insufficient data about CT imaging of animal vesicular glands, particularly in rabbits, motivated the present investigation on some anatomo-topographic features of these organs using computed axial tomography.

These data could be used as a reference background in diagnostics for the differentiation of healthy from pathologically altered vesicular glands in this animal species in which the incidence of squamous metaplasia, hyperplasia and vesicular glands keratinization is estimated to approximately 45% as reported by Zwicker *et al*. (1985) in New Zealand white rabbits.

MATERIALS AND METHODS

Eight sexually mature, clinically healthy male white New Zealand rabbits, aged 12 months and weighing

Corresponding Author: R. Dimitrov, Department of Veterinary Anatomy, Histology and Embryology,
Faculty of Veterinary Medicine, Trakia University, 6000 Stara Zagora, Bulgaria

2.8-3.2 kg were used in this study. The animals were anesthetized with 15 mg kg^{-1} Zoletil® 50 (tiletamine hydrochloride 125 mg and zolazepam hydrochloride 125 mg in 5 mL of the solution) Virbac, France.

The experiment was performed in strict compliance with the ethical guidelines for humane treatment of animals as defined by the European convention for the protection of vertebrate animals used for experimental and other scientific purposes, the European Convention for the protection of pet animals and Law on Animal Protection in the Republic of Bulgaria-part IV (Animal Experimentation).

Three animals were positioned in ventral recumbency and the other five in dorsal recumbency. In two animals the CT imaging was precontrasted, in another three the contrast enhancement was done with Optiray® 350 (ioversol 741 mg mL^{-1}), Healthcare Ltd., UK and in the last three rabbits with Urografin 76% (sodium amidotrizoate 0.1 g mL^{-1} and meglumine amidotrizoate 0.66 g mL^{-1}), Schering Ltd., Germany. Optiray® 350 was administered intravenously at 1 mL kg^{-1} in the cephalic vein and the investigation was performed immediately. The second contrast agent Urografin 76% was applied orally as a 1.52% aqueous solution (30 mL kg^{-1}, fractional administration) aiming better differentiation of rectum toward vesicular glands. The imaging was performed 3 h later. Transverse scans of the pelvic area were performed by means of an axial computed tomograph SIEMENS, SOMATOM, ARTX with FOV = 250, filter 1, 70 mA and 110 kV. Each scanning time was 3 sec. A high-resolution 512 mode, gantry tilt of 0° was employed with window width and centre 280 and 53. Scans were done at 2 mm intervals and section thickness was 2 mm.

For defining the topography of the rabbit vesicular glands, the following osseous markers were used: the lumbar and sacral vertebrae (dorsally), the abdominal wall or the cranial branch of the pubic bone (ventrally) and the body of the ilium (laterally). The transverse CT scans of the pelvis were performed in the transverse planes between L7 and S1 and up to the caudal end of S1. The cranial CT scans were bounded laterally by the body of the ilium extending between the sacroiliac joint and the acetabulum, ventrally by the abdominal wall and dorsally by the plane between the seventh lumbar vertebra and the beginning of the first sacral vertebra. The caudal CT scans were marked laterally by the body of the ilium near to the acetabulum, ventrally by the cranial branch of the pubic bone and dorsally by the end of the first sacral vertebra. The selected soft tissue markers were the well-visualized urinary bladder neck (both in precontrast and postcontrast images), the beginning of the pelvic urethra and the rectum (precontrast images).

Three-dimensional image reconstruction was made by Multiplanar reformating program in order to obtain reconstructed images of the pelvic organs within in dorsal and sagittal views. The statistical processing of data was made by statistical software (StatMost for Windows, 1994).

RESULTS

Dorsal and sagittal views of the reconstructed CT images of the rabbit vesicular glands and the surrounding bone and soft tissue structures are shown in Fig. 1 and 2. The vesicular glands are relatively large, homogeneous soft tissue structures situated dorsolaterally to the contrast enhaced beginning of the pelvic urethra. The glands are located at the pelvic inlet, cranially to the cranial part of the voluminous prostatic gland which is characteristic of rabbits. The vesicular glands are relatively large, homogeneous soft tissue structures situated dorsolaterally to the beginning of the pelvic urethra (Fig. 1 and 2).

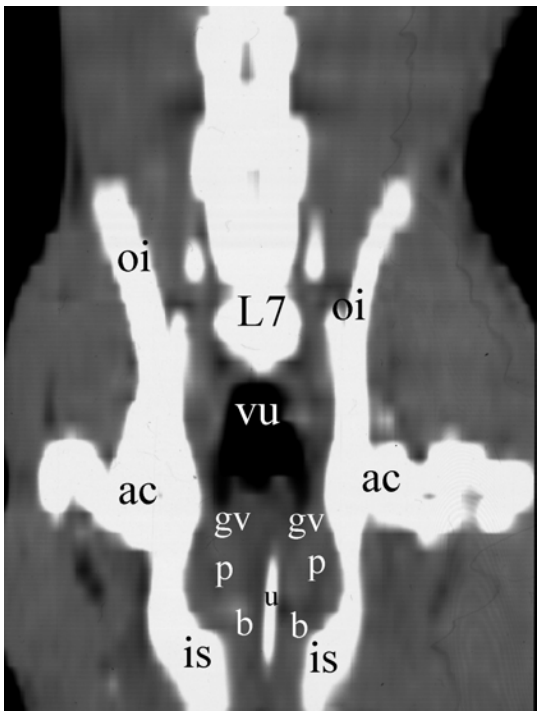

Fig. 1: Reconstructed postcontrast (Optiray® 350) CT image of the accessory genital glands and pelvic urethra in the rabbit (dorsal view): vesical blader (vu), vesicular glands (gv), prostate complex (p), pelvic urethra (u), bulbourethral glands (b), body of ilium (oi), acetabulum (ac), ischium (is), seventh lumbar vertebrae (L7)

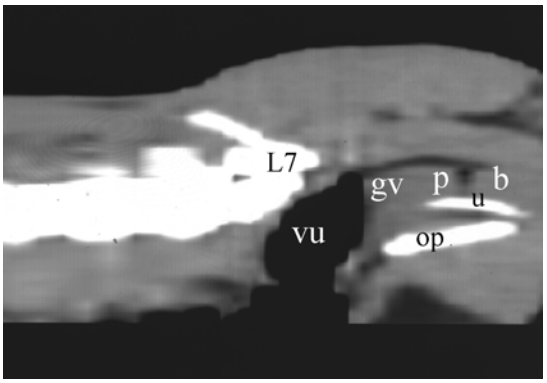

Fig. 2: Reconstructed postcontrast (Optiray® 350) CT image of the accessory genital glands and pelvic urethra in the rabbit (sagittal view): vesical blader (vu), vesicular glands (gv), prostate complex (p), pelvic urethra (u), bulbourethral glands (b), seventh lumbar vertebrae (L7), pubis (op)

Fig. 3: Transverse postcontrast (Optiray® 350) CT image of the rabbit pelvis at the cranial border of S1 in dorsal recumbency. CT scans thickness 3 mm: urinary bladder neck (cv), vesicular glands (glv), rectum (r), body of ilium (oi), femur (f)

The transverse CT image of the pelvis on scans made between L7 and S1 (Fig. 3) depicts the body of the ilium (laterally), the absence of any bone marker (ventromedially) and the beginning of S1 (dorsally). In the pubic region, the contrast-enhanced urinary bladder neck is observed. Its lumen is hyperdense and its wall is relatively hypodense and homogeneous. Dorsally to the neck, beneath the rectum, the beginning of vesicular

Fig. 4: Transverse precontrast CT image of the rabbit pelvis through the middle of S1 in sternal recumbency. CT scans thickness 3 mm: transition between urinary bladder neck and pelvic urethra (cv), vesicular glands (glv), rectum (r), body of ilium (oi), femur (f)

glands is visualized as soft tissue structures that are relatively hypodense as compared to the urethral and rectal walls. The first appearance of the CT image of rabbit vesicular glands was in the transverse plane between L7 and S1, the body of the ilium and the ventral abdominal wall.

The major CT image of the vesicular glands was obtained in scans done in the transverse plane through the middle of S1 where the lumen of the pelvic urethra was not contrast-filled (hypodense). The glands were visualized as hypodense soft tissue structures located at the pelvic inlet between the urethra and the rectal wall (Fig. 4). The vesicular glands were differentiated from prostate gland only by their anatomo-topographic traits as both exhibited similar soft tissue characteristics. Both the urethral and rectal walls were hyperdense as compared to the glandular appearance.

At the caudal end of S1, the caudal parts of the vesicular glands were seen in native CT images as soft tissue structures situated above the pelvic urethra, medially to the body of the ilium and craniomedially above the pelvic brim (Fig. 5). The vesicular glands area was relatively hypodense against the urethral wall.

The average transverse lateromedial diameter of glands was 5.48±0.03 (mean±SEM; range 5.4-5.6) mm, a dorsoventral height of 4.6±0.02 (range 4.5-4.6) mm and a craniocaudal length of 6.2±0.02 (range 6.2-6.3) mm. The density of the rabbit vesicular glands demonstrated a soft

Fig. 5: Transverse postcontrast (Urografin 76%) CT image of the rabbit pelvis through the caudal part of S1 in ventral recumbency. CT scans thickness 3 mm: beginning of the pelvic urethra (cv), vesicular glands (glv), rectum (r), body of ilium (oi), femur (f)

tissue character, ranging from 31±0.33 (range 31-33) HU in precontrast imaging and 78±0.33 (range 78-80) HU in postcontrast imaging. There were no anatomo-topographic differences in the location of the vesicular glands between animals in dorsal and sternal recumbency in the study.

DISCUSSION

Via the computed tomography, we have demonstrated *in vivo* that the topography of rabbit vesicular glands was similar to that described previously by post mortem anatomical methods (Del Sol and Vasquez, 2003; Holtz and Foote, 1978; McCracken *et al*., 2008). The present CT imaging study shows not only the localization, size and shape of the glands but also its relationships with the adjacent structures.

The vesicular glands of the rabbit have a tissue density, similar to that of the human vesicular glands (Silverman *et al*., 1985; Kuyumcuoglu *et al*., 1991; Altunrende *et al*., 2004; Lawson and Macdougall, 1965) but they are homogeneous structures, in contrast to the heterogeneous image in humans (Lantz *et al*., 1981).

In this *in vivo* CT imaging study, all three dimensions of the rabbit vesicular glands (width, height, length) are presented for quantitative evaluation purposes. This contrasts with the reports of Munkelwitz *et al*. (1997) who described gland length and width as a sign of vesicular dilatation in humans and Archana *et al*. (2009) who studied post mortem age-related differences in gland size in goats. Both dorsal and sternal recumbencies were equally definitive positions for vizualisation the rabbit vesicular glands as compared to the man where only the dorsal one is used (Altunrende *et al*., 2004; Lawson and Macdougall, 1965).

The application of the ionic monomeric contrast medium Urografin 76% with regard to the definitive visualization of the studied soft tissue findings did not imporve the quality of the image which according to us was due to the lower absorption of the contrast agent from the tissues, after peroral application. The non-ionic monomeric contrast agent Optiray® 350, applied intravenously was more appropriate for computed tomography investigation of the rabbit vesicular glands.

CONCLUSION

The results from the computed tomography imaging of the rabbit vesicular glands could be used as a reference background for the diagnosis and interpretation of various pathologies in this animal species.

Furthermore, the diagnostic imaging of the adjacent urinary bladder neck and the beginning of the pelvic urethra by means of CT could be successfully used for investigation of anatomic characteristics and abnormalities of these organs including diverticula, stenosis, lithiasis and cysts of the urinary tract.

REFERENCES

Altunrende, F., E. Kim, F. Klein and W. Waters, 2004. Seminal vesicle cyst presenting as rectal obstruction. Urol., 63: 584-585.

Archana, P., R. Katiyar, D. Sharma and M. Farooqui, 2009. Gerontological studies on the gross and histomorphology of the vesicular gland of Gaddi Goat (*Capra hircus*). Int. J. Morphol., 27: 13-20.

Del Sol, M. and B. Vasquez, 2003. Mesoscopy and histology of the vesicular gland in the (*Orictolagus cuniculus*). Int. J. Morphol., 21: 325-330.

Holtz, W. and R. Foote, 1978. The anatomy of the reproductive system in male Dutch rabbits (*Oryctolagus cuniculus*) with special emphasis on the accessory sex glands. J. Morphol., 158: 1-20.

Kang, Y.S., E. Fischman, J. Kuhlman and S. Goldman, 1989. Seminal vesicle abscesses: Spectrum of computed tomographic findings. Urol. Radiol., 11: 182-185.

Kuyumcuoglu, U., D. Erol, C. Germiyanoglu and L. Baltaci, 1991. Hydatid cyst in the seminal vesicle. Int. Urol. Nephrol., 23: 479-483.

Lantz, E.J., T.H. Berquist, R.R. Hattery, M.J. Mattson and M.M. Lieber, 1981. Seminal vesicle cyst associated with ipsilateral renal agenesis: A case report. Urol. Radiol., 2: 265-266.

Lawson, L. and J. Macdougall, 1965. Multilocular cyst of the seminal vesicle. Br. J. Urol., 37: 440-442.

Lee, B., J. Seo, Y. Han, Y. Kim and S. Cha, 2007. Primary mucinous adenocarcinoma of a seminal vesicle cyst associated with ectopic ureter and ipsilateral renal agenesis: A case report. Korean J. Urol., 8: 258-261.

McCracken, T., R. Kainer and D. Carlson, 2008. Color Atlas of Small Animal Anatomy: The Essentials. Blackwell Publishing, USA., pp: 160.

Mollineau, W., A. Adogwa, N. Jsaper, K. Young and G. Garcia, 2006. The gross anatomy of the male reproductive system of a neotropical rodent: The agouti (*Dasyprota leprina*). Anatomia Histol. Embryol., 35: 47-52.

Munkelwitz, R., S. Krasnokutsky, J. Lie, S. Shah, J. Bayshtok and S. Khan, 1997. Current perspectives on hematospermia: A review. J. Androl., 18: 6-14.

Silverman, P., N. Dunnick and K. Ford, 1985. Computed tomography of the normal seminal vesicles. Comput. Radiol., 9: 379-385.

StatMost for Windows, 1994. DataMost Corporation. StatMost Publisher, USA., pp: 87-96.

Zwicker, G., J.M. Killinger and R.F. McConnel, 1985. Spontaneous vesicular and prostatic gland epithelial squamous metaplasia, hyperplasia and keratinized nodule formation in rabbits. Toxicol. Pathol., 13: 222-228.